

## Counter versus Co Tangential Neutral Beam Injection Performance on the Mega Ampere Spherical Tokamak

R.J.Akers, P.Helander, M.R.Tournianski, C.Brickley, N.J.Conway, A.Field, A.Kirk, D.Muir, A.Patel and the MAST and NBI teams.

EURATOM/UKAEA Fusion Association, Culham Science Centre,  
Abingdon, Oxon, OX14 3DB, UK

Auxiliary heating of the MAST spherical tokamak (ST) is provided by two, tangentially orientated ( $R_T=0.7m$ ) Neutral Beam Injectors, typically delivering  $\sim 3MW$  of highly collimated, 40keV neutral deuterium. The resulting fast ion orbits, which border on non-adiabaticity due to the low magnetic field of the ST plasma, are modelled using two NBI codes - the Larmor orbit corrected guiding centre tracker within TRANSP and the full gyro orbit code LOCUST. In this paper we compare the plasma performance of a series of counter injection heated discharges (shown throughout as solid red circles), against typical co-injection heated plasmas (shown as black squares).

Co-injection on MAST is well documented [1], LOCUST and TRANSP model predictions agreeing well with measured neutron rates and stored energy (see for example Figs.1a and b), plasma surface voltage and diamagnetic flux, indicating fast ion absorption efficiency close to 100% and plasma resistivity in agreement with neoclassical theory. In addition, fast ion spectra sampled using a horizontally scanning neutral particle analyser are in good agreement with both LOCUST and TRANSP predictions, indicating that fast ions are scattered predominantly by multiple small-angle Coulomb scattering, thus lending credence to the modelled level of Neutral Beam Current Drive (NBCD).

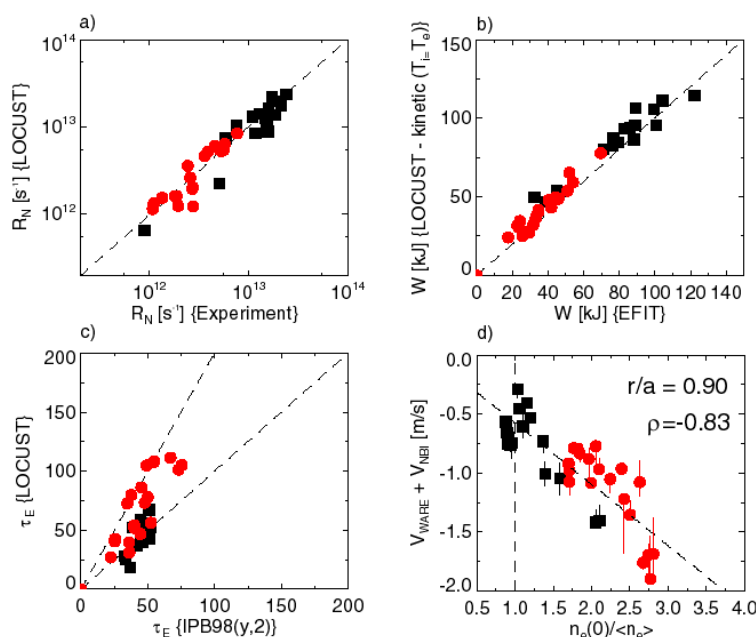


Fig. 1: Simulated vs. measured neutron rate, kinetically determined stored energy vs. EFIT, measured confinement time vs. scaling IPB98[y,2] and pinch velocity vs.  $n_e$  peaking factor, for the co- (black) and counter- (red) NBI heated discharges used in this study.

heated discharges). Although deposited deep inside the plasma, many of the trapped fast ions become promptly lost due to charge exchange in the molecular gas blanket surrounding the plasma (where  $n_{D_2} \sim 10^{18} m^{-3}$ ) or through collisions with the poloidal field coils and

Counter-injection is of current interest due primarily to the discovery of QH-mode, a means by which high performance ELM free operation can be achieved. Counter-NBI can also, however, be used as a valuable tool for testing NBI heating and transport models.

Unfortunately, on MAST, both modelling and experiment indicate that only  $\sim 30-50\%$  of the fast ion energy is absorbed using counter-NBI. This results in significantly reduced neutron rates (Fig.1a) and power flow to the target Langmuir probes (which can be reduced by as much as a factor of  $\sim 4$  compared with co-NBI

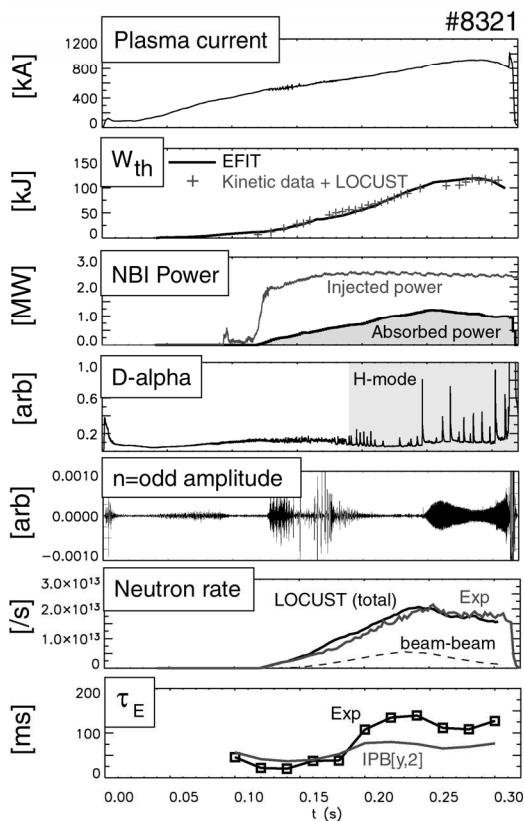


Fig. 2: Experimental and model data for counter NBI H-mode discharge #8321.

with LOCUST model predictions for counter NBI heated discharge #8321, a 120kJ high performance H-mode plasma. Here, toroidal rotation (~300-340km/s in the core) was determined from the outboard-inboard asymmetry in the TS density profile, consistent with levels extracted from charge exchange recombination spectroscopy. The  $Z_{eff}$  profile, measured using a 2D Bremsstrahlung imaging diagnostic, is similarly skewed towards the low field side, and is modelled well by theory (Fig. 3) where:

$$\frac{n_z}{n_{z0}} = \exp \left[ \left( 1 - \frac{T_e}{T_i + T_e} Z \frac{m_i}{m_z} \right) \frac{m_z \omega^2 (R^2 - R_0^2)}{2T_z} \right], \dots\dots\dots [1]$$

consistent with the assertion that the dominant impurity on MAST is fully stripped Carbon (also confirmed by spectroscopy). The confinement  $H_H$  factor (with respect to ITER scaling IPB98[y,2]) is ~2.0 in H-mode (dropping slightly with the onset of large ELMs and tearing activity), i.e. double that for typical co-NBI heated, quiescent H-mode discharges. Equally as striking, electron density profiles are routinely much more peaked (with little or no evidence of edge density "ears") and temperature profiles are much broader than for co-injection. Fig. 4 shows a scatter plot of density versus temperature profile peaking factor for a number of co- and counter- NBI heated discharges using the MAST 300 point Thomson scattering (TS) system, highlighting the different character of the profiles.

Similar results have been reported at Large Aspect Ratio, on ASDEX [2] where confinement was seen to double with counter NBI, concurrent with peaking of the density profile, and on JFT-2M [3] where it was suggested that density peaking may have been due to the presence of a "turbulence driven" pinch.

protection armour. In contrast to the absorbed power, however, the angular momentum delivered to the plasma is predicted to be somewhat "larger" with counter- compared with co-NBI due to the rapid loss of predominantly "co-moving" NBI ions. This results in an increase of ~30% in the applied torque for  $P_{inj} \sim 1\text{MW}$ , rising to ~50% at 2.5MW where the highest counter-NBI performance is achieved. It is not surprising therefore that the observed plasma rotation using counter NBI on MAST, is equal to, if not greater than that of co-injected discharges, with core rotation speeds greatly exceeding the Carbon thermal velocity and approaching the plasma sound speed.

Perhaps even more notable is that even with a reduction in auxiliary heating power of >50%, a number of counter NBI heated plasmas exhibit thermal stored energies comparable to those for the highest performance co-injection discharges; counter-NBI ELMing and ELM free H-mode are for example readily accessed (possibly due to the larger angular momentum injection) with acceptably low  $Z_{eff}$  (typically ~2-3). Fig. 2 shows experimental data together

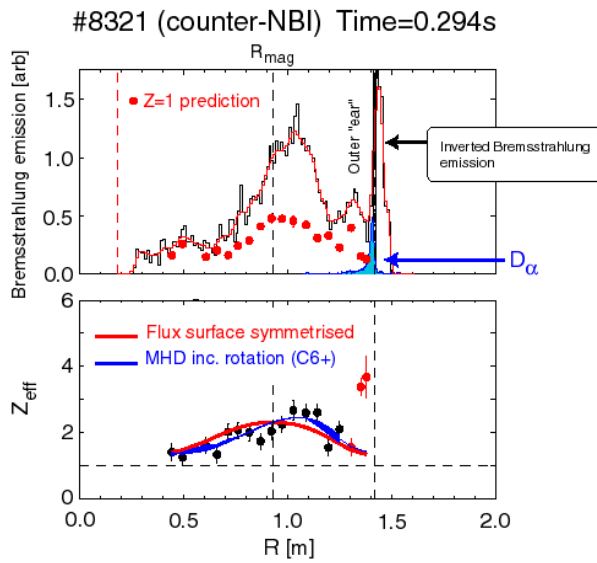


Fig.3: Bremsstrahlung emission and the resulting  $Z_{eff}$  for counter-NBI discharge #8321 @294ms.

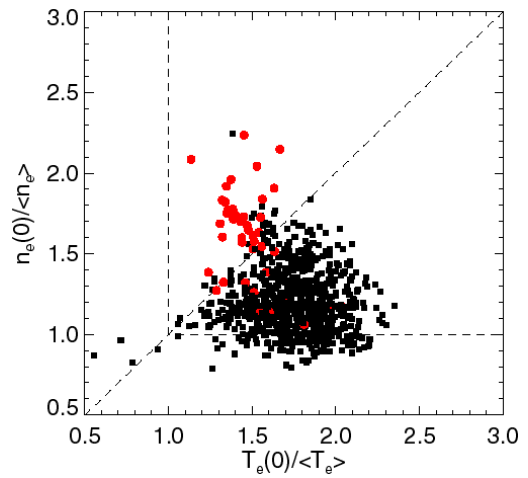


Fig.4:  $n_e(0)/\langle n_e \rangle$  vs.  $T_e(0)/\langle T_e \rangle$ , highlighting the different character of co (black) and counter (red) discharges.

No mention was made in either paper, however, of the neoclassical Ware pinch. For co-NBI heated MAST discharges,  $Z_{eff}$  is routinely flat and very close to 1.0. Counter NBI heated discharges on the other hand are, as already noted, considerably less pure (perhaps due to sputtering of Carbon from the upper P2 armour plate where the fast ion up-down asymmetric load is predicted to be of order  $\sim 2 \times 10^{19}/s$ ). A larger loop voltage is thus required to sustain the plasma current, which in turn drives a larger Ware pinch. Using the formalism of [4] one can express the full neoclassical pinch, applicable to arbitrary aspect ratio and shaped toroidal plasmas, in terms of the transport coefficients  $l_{13}^e$  and  $l_{11}^e$ :

$$\begin{aligned}
 & \text{NBCD DRIVEN PINCH} \\
 \langle \vec{\Gamma}_e \cdot \nabla \psi \rangle^{\text{pinch}} &= \frac{I}{m_e \Omega_0^2 \tau_e} \left[ \frac{\ell_{13}^e Z_f}{Z_{eff}} \langle j_f B \rangle + \frac{1}{1 + \nu_*} \frac{Z_f / Z_{eff}}{\langle B^{-2} \rangle} \left( \langle \frac{j_f}{B} \rangle - \langle \frac{1}{B^2} \rangle \langle j_f B \rangle \right) \right. \\
 & \quad \left. - \frac{\ell_{13}^2}{\langle B^2 \rangle \langle B^{-2} \rangle} \frac{n_e e^2 \tau_e}{m_e} \langle E_{\parallel} B \rangle \right] \\
 & \text{WARE PINCH} \dots\dots\dots [2]
 \end{aligned}$$

where  $\psi$  is the poloidal flux function. The last part of Eqn. 2 is the Ware pinch with the first and second terms comprising an NBCD driven pinch (due to friction between the NBI ions and thermal electrons, proportional to the unshielded beam driven current  $\langle j_f B \rangle$ ). The fast ion driven pinch is thus in the same direction as the Ware pinch for counter-injection but acts radially outwards for co-injection. For the discharges used in this analysis, we note that the NBCD is a small fraction of the ohmically driven current (typically  $<10\%$ ), resulting in the Ware pinch being dominant for all but the very centre of the plasma. This will cease to be the case of course, as beam power is increased towards the design goal of 5MW and low density, NBI driven steady state operation becomes routine.

As well as neutron rate and stored energy, Fig.1 shows c), confinement time versus scaling IPB98[y,2], highlighting the high performance of many counter-NBI discharges and d),

pinch velocity versus density profile peaking factor at  $r/a \sim 0.9$  (where there is good confidence in  $\psi(R,Z)$  from EFIT). There is clearly a strong correlation between peakedness of the density profile and strength of the inwards neoclassical pinch (correlation coefficient  $\rho=0.83$ ), hinting that the Ware pinch plays a key role in defining the shape of the density profile (indeed, more so than the change attributed to L-H transition). It is important to note that the pinch velocity calculation is solely dependent upon the EFIT solution, i.e., independent of the TS data, thus ruling out any diagnostic systematic correlation. The regression correlation coefficient in the core reduces steadily to 0.67 at  $r/a \sim 0.5$  and 0.30 at  $r/a \sim 0.3$ , most likely as a result of decreasing confidence in  $\psi(R,Z)$ .

In order to achieve greater accuracy in the plasma core, work is currently underway to implement Eqn.2 in TRANSP, thereby allowing the poloidal field diffusion equation to be solved to determine  $\psi(R,Z)$ , thus providing a more accurate value of  $\langle E_{\parallel} B \rangle$ . This is possible as both ohmically and NBI heated plasmas show good agreement between the measured surface voltage (using EFIT and magnetics) and values predicted by TRANSP assuming neoclassical resistivity. Preliminary results indicate that the Ware pinch formula already implemented in TRANSP is, however, satisfactory for MAST for  $r/a > 0.4$ . Recalling the observation that the NBCD driven pinch for the discharges under consideration is small (the NBI pinch being absent in TRANSP), it is thus possible to deploy the currently available model. Fig.5 shows the equivalent of Fig.1d) at  $r/a=0.5$ , this time using TRANSP, with a corresponding correlation coefficient of 0.84. At this radius, on average, the beam electron source exceeds the edge fuelling source (which is constrained by mid-plane  $D_{\alpha}$ -array, Langmuir probe and TS data), providing a reasonable level of confidence in the resulting magnitude of electron diffusion. Due to unknown poloidal variation in gas fuelling, and inaccuracies in the measured pedestal density and temperatures, it is difficult to extract absolute values for individual discharges. It is sufficient, however, to note that best estimates for the diffusion coefficients ( $D < 0.25 \text{ m}^2/\text{s}$ ) correspond to radial velocities  $< 1 \text{ m/s}$ , i.e., consistent with the Ware pinch being strong enough to have a profound influence upon the electron particle flux.

It is well established that peaked density profiles and strong rotational shear act to stabilise micro-instabilities. It is plausible therefore, that density peaking during counter-NBI, driven by the increased Ware pinch, and combined with an increased contribution to the ExB flow-shear (due to the prompt loss of trapped fast ions during their co-orbital leg), act together to reduce energy and particle transport, resulting in  $H_H$  factors of order  $\sim 2.0$  and broad, rather than peaked, temperature profiles.

[1] R.J.Akers et al., Plasma Phys. Control. Fusion **45** (2003) A175-A204.

[2] O.Gehre et al., Phys. Rev. Lett. **60** 15 (1988) 1502.

[3] K.Ida et al., Phys. Rev. Lett. **68** 2 (1992) 182.

[4] O.Sauter and C.Angioni, Phys of Plas **6** 7, 2834 (1999).

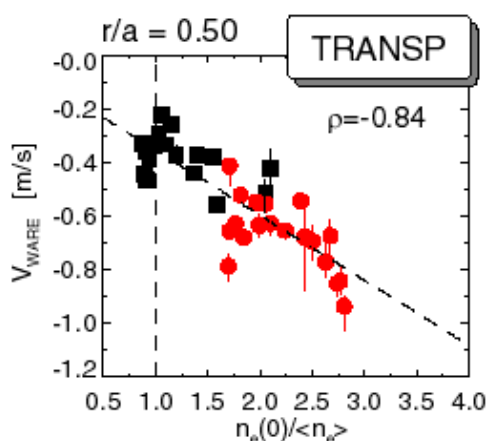


Fig. 5: Ware pinch velocity vs. electron density peaking factor at  $r/a=0.5$  using TRANSP.